IEEE Access
Multidisciplinary | Rapid Review | Open Access Journal

Received June 16, 2020, accepted July 21, 2020, date of publication July 24, 2020, date of current version August 5, 2020.

Digital Object Identifier 10.1109/ACCESS.2020.3011750

Novel Piezoelectric Emergency Opening Sub-System to Improve the Safety and Reliability of Zero-Holding-Energy Permanent Magnet Magnetic Contactors

NIKITA GABDULLIN, (Member, IEEE), AND JONG-SUK RO, (Member, IEEE)
School of Electronic and Electrical Engineering, Chung-Ang University, Seoul 06974, South Korea

Corresponding author: Jong-Suk Ro (jongsukro@gmail.com)

This work was supported in part by the Basic Science Research Program through the National Research Foundation of Korea funded by the Ministry of Education under Grant 2016R1D1A1B01008058; and in part by the Chung-Ang University Research Grants, in 2018.

ABSTRACT Conventional switchgear such as relays and magnetic contactors (MC) continuously consume energy to maintain an open and/or closed state, contributing to unnecessary energy consumption, dissipation, and heating. The minimization of such losses has become an important topic in recent years, leading to the development of more energy-efficient technologies such as permanent magnet (PM) MCs. However, concerns regarding the safety and reliability of PM MCs hindered the development of a zero-holding-energy PM MC (ZMC) due to the loss of the controllability in emergency scenarios (such as power outages). This paper presents a novel piezoelectric emergency subsystem (PES) that monitors the state of the input power source and opens the ZMC in emergency circumstances. The proposed PES consumes no energy upon charging its piezoelectric element, thus allowing the holding energy of the complete ZMC-PES system to remain zero without affecting the normal operating regimes of the ZMC. Because the application of the PES causes the ZMC to act as a normally-open MC, the ZMC-PES system can be conveniently controlled using traditional solenoid MC control strategies, enabling an easy transition from the conventional to the proposed technologies. The feasibility of the proposed PES is verified using data obtained from a fabricated prototype of a complete ZMC-PES system. The proposed system is promising not only for industrial grids, but also for vehicular microgrids as in electric aircrafts and ships where energy efficiency translated into the increased battery lifetime.

INDEX TERMS Emergency sub-system, magnetic contactor, permanent magnet, piezoelectric cantilever, zero-holding-energy.

I. INTRODUCTION

Increasing the efficiency of electrical energy generation and distribution, as well as reducing overall energy consumption, has become a crucial research topic in recent decades. This is particularly important for the industrial sector, which in the US, contributes to more than 30% of the total energy consumption [1]. Furthermore, electric power generation and manufacturing industries contribute up to 40% of the global CO_2 emissions [2]. Conventionally, researchers have been primarily focused on improving the efficiency of energy generation and conversion. However, in recent years the efficiency of energy distribution and consumption has been gaining increasing attention. Specifically, improving the energy efficiency of devices that connect consumers in electrical grids, such as relays and magnetic contactors (MCs), has the potential to eliminate one source of energy consumption completely, namely the energy consumed by an MC while maintaining a closed state (holding energy). Efforts to achieve zero-holding-energy devices have led to the development of permanent magnet (PM) MCs. However, these new designs have not yet achieved both sufficient energy efficiency and reliability in a single device.

In addition to conventional industrial applications of MCs, energy efficient MCs are important for vehicular microgrids ranging from small electric car grids to larger AC and

The associate editor coordinating the review of this manuscript and approving it for publication was Jenny Mahoney.

DC grids of electric ships and aircrafts [3], [4]. Similar reasoning also applies to high-efficiency renewable energy utilization relevant for windfarm grids [5], [6].

Previously Fang *et al.* [7] and Shu *et al.* [8] have developed PM MCs with stationary magnets that reduce the energy consumption and show improved dynamic characteristics. Wang *et al.* have shown the feasibility of PM MCs for voltages as high as 126 kV [9]. However, such PM MCs require a non-zero holding current. Thus, these PM MCs are also subjected to common drawbacks of solenoid MCs such as vibration and unstable contact positioning that hinder their reliability [10].

Bak *et al.* [11] proposed an electronically-controlled PM MC in which the holding energy is consumed only by the electronic components. Recently, Gabdullin and Ro [12] developed a zero-holding-energy MC (ZMC) that required no holding current and used no active electronic components. However, the ZMC had an important reliability issue that caused the loss of controllability in the case of a power outage, giving rise to a number of potentially harmful scenarios. In the absence of an emergency power supply, a closed ZMC is impossible to open after a power outage. As a result, when power is restored all consumers are instantaneously connected to the grid causing a potentially devastating overload [13]. Furthermore, the sudden starting of rotating machines can pose a danger to personnel. Therefore, the development of a normally-open ZMC is desired to ensure the safety and reliability of the system.

However, the development of a normally-open ZMC poses fundamental challenges. In a power outage scenario, control signals cannot be sent and devices that require input energy to open a ZMC (such as solenoid actuators) cannot be used. Furthermore, conventional monitoring systems that continuously consume energy are not appropriate for a zero-holding-energy system. Hence, a technology is desired that is able to store sufficient energy and release it to achieve emergency opening in the case of a power outage. Furthermore, such technology must consume no additional energy to preserve the stored energy. This technology must also have a rapid automatic response, on the order of milliseconds, to ensure the safety of the grid and personnel. Novel smart materials, such as shape memory alloys (SMA) or magnetic shape memory alloys (MSM), comply with the energy storage requirements but require a control signal for activation in emergency situations [14], [15].

This paper proposes a sub-system that satisfies the aforementioned requirements and monitors the supply voltage to react instantly when the input voltage is removed. The proposed piezoelectric (PZT) emergency sub-system (PES) consists of a PZT cantilever bender (PB), a 45 VDC battery, and a rectifier. Piezoelectric actuators, especially PBs, have previously been widely applied as high-frequency resonance mechatronic devices [16]–[18], energy harvesters [19]–[22], and high-precision sensors [23], but their application as DC zero-energy-consumption macro-switch elements has not been studied in detail. The implementation of the proposed PES allows the ZMC to act as a normally-open MC, while the ZMC-PES system satisfies the zero-holding-energy requirement. Furthermore, the lifetime of the battery is extended because the PES only consumes battery energy under emergency circumstances, hence resulting in a reliable, energy-efficient, and cost-effective technology.

II. DESIGN AND ANALYSIS OF THE PROPOSED PES

A. INVESTIGATING THE POSSIBILITY OF DESIGNING A ZERO-HOLDING-ENERGY PES

The desired sub-system for emergency opening of ZMCs should comply with the operating principles shown in Fig. 1. When the input power is available, the subsystem should store the required energy and be on standby while consuming no additional energy. Furthermore, it must not affect the normal operating of the ZMC. On the other hand, in the case of a power outage, the sub-system should release the stored energy and open the ZMC to disconnect its load.

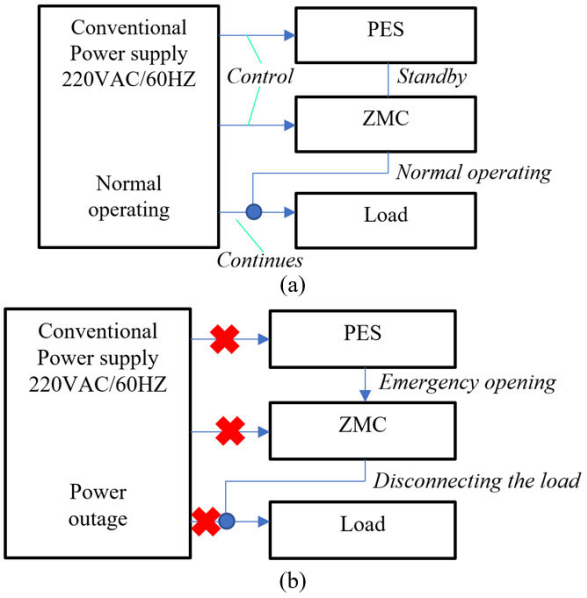

FIGURE 1. (a) Normal operating of PES-ZMC system and (b) emergency opening in case of power outage.

This study investigates the feasibility of a PZT-based subsystem as a solution to the challenge of achieving safe and reliable ZMCs. PZT elements are commonly used for micropositioning [24], [25] or high-frequency ultrasonic applications rather than bulk macroscopic motion [26]–[28]. For the latter purpose, preloaded PZT stack actuators can be used, although they provide large forces for an extremely limited displacement [29]. Furthermore, PZT actuators are commonly used in resonance conditions for stroke amplification [16]–[18], [30]. Unfortunately, these solutions cannot be applied to solve the power outage scenario examined by this study due to the unavailability of an energy source in the case of a power outage, which makes the resonance-mode utilization unsuitable. However, PBs can be used to increase the displacement at expense of stiffness and output force.

Furthermore, PBs respond to a DC voltage and maintain their deformation, acting as a monitoring element.

The proposed PES takes advantage of the ability of PZT materials to deform when storing electric charge [31]. PZT switches of this type have been proposed; yet, they are less known than other piezoelectric actuators [32]. Hence, the PZT element acts as a capacitor with infinite impedance when connected to a DC circuit, as shown by the denominator in (1). Hence, a PZT element in a DC circuit prevents any further charge or power ($P_{PB(hold)}$) in (1)) from being transferred after it is charged, and the voltages in the circuit are balanced as shown in Fig. 2. This ensures that energy is consumed by the PES only when charging the PB, and the PB maintains its deflection at constant voltage with no further energy consumption.

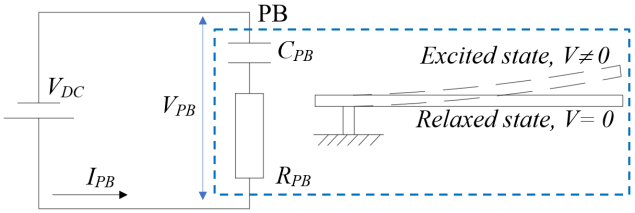

FIGURE 2. Response of a PB to a DC voltage (V_{DC}), maintaining a deformed state with no energy consumption. V_{PB}, R_{PB}, I_{PB}, and C_{PB} are the voltage, resistance, current, and capacitance of the PB, respectively.

The state of the PB is described by

$$P_{PB(hold)} = I_{PB}V_{DC} = \frac{V_{DC}^2}{Z_{PB}} = \frac{V_{DC}^2}{\sqrt{R_{PB}^2 + \frac{1}{\omega C_{PB}}^2}} \to 0 \quad (1)$$

$$\delta_{tip} = f\left(l_s, l_p, h_s, h_p, d_{31}, Y_s, Y_p, V_{DC}\right) \quad (2)$$

where δ_{tip} is the displacement of the PB's tip, Y_s and Y_p are the Young's moduli of the metal shim and PZT layers, respectively, and d_{31} is the transverse piezoelectric constant. The geometrical parameters of the PB are shown in Fig. 3. Solving (2) is discussed in the next subsection.

The PB does not produce enough force to open the ZMC, and a 45 VDC battery is used for that purpose as discussed in detail in Section III. Instead, the PB controls a contact that connects or disconnects the battery to the ZMC. Therefore, the PB acts as a zero-holding-energy monitoring element for the input voltage, instantaneously reacting to a loss of voltage, which is essential for a prompt response in power outage circumstances.

B. DESIGN AND ANALYSIS OF THE PB FOR PES

Whereas (2) shows a general expression for δ_{tip}, obtaining an exact analytical solution is a rather complex problem. Finding the deflection of a PZT cantilever tip with high precision requires a complex system of differential equations to be solved, and even simplified models are rather difficult to analyze [25], [33]–[35]. Moreover, analyzing coupled electro-mechanical behavior of PB requires both electrical and mechanical sub-systems to

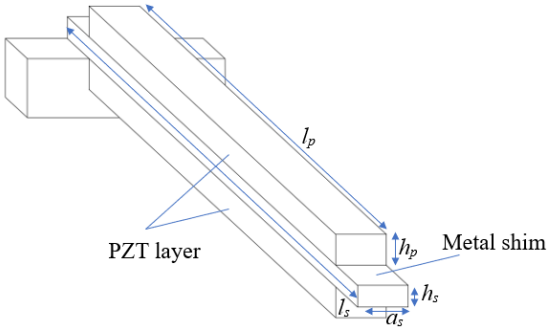

FIGURE 3. Structure of the bimorph PB showing its geometrical parameters.

be considered simultaneously [20], [36], [37]. Obtaining an analytical solution for PZT structures more complex than the bimorph PB shown in Fig. 3 further complicates the problem, as in case of pre-strained cantilevers [38]. However, numerical methods could ensure accurate analysis and substantially reduce the analysis time when complex structures are considered [39], [40].

Thus finite element analysis (FEA) was employed in this study using JMAG software as shown in Fig. 4 to ensure large macroscopic tip displacement of PBs. To evaluate PB tip displacement, zero displacement boundary conditions were applied at the fixed end of the PB while other PB parts remained free. PB excitation was modeled by applying 60 − 300 V to each PZT layer and zero voltage to the metal shim. The PZT material was Lead Zirconate Titanate PZT-5A with density 7500 kg/m^3. PZT-5A was chosen as affordable high sensitivity and permittivity material with very high piezoelectric coupling factor [41]. It also has better thermal stability compared to other piezoceramics which is extremely important for industrial applications where ambient temperature can vary greatly and prolonged operating without performance deterioration is required [42]. The parameters of PZT layers are

$$E_p = \begin{bmatrix} 12 & 7.52 & 7.51 & 0 & 0 & 0 \\ 7.52 & 12 & 7.51 & 0 & 0 & 0 \\ 7.51 & 7.51 & 11.1 & 0 & 0 & 0 \\ 0 & 0 & 0 & 2.1 & 0 & 0 \\ 0 & 0 & 0 & 0 & 2.1 & 0 \\ 0 & 0 & 0 & 0 & 0 & 2.26 \end{bmatrix} \quad (3)$$

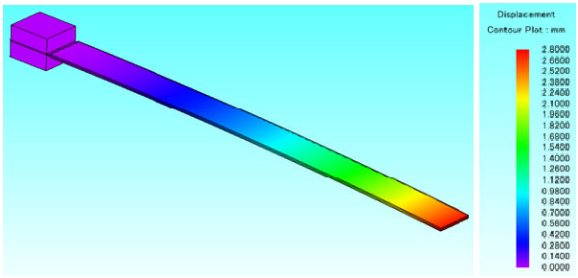

FIGURE 4. Deformation of a PB in response to the applied DC voltage, analyzed using JMAG.

$$e = \begin{bmatrix} 0 & 0 & 0 & 0 & 12.3 & 0 \\ 0 & 0 & 0 & 12.3 & 0 & 0 \\ -5.3 & -5.3 & 15.8 & 0 & 0 & 0 \end{bmatrix} \quad (4)$$

where E_p is stiffness matrix in 10^{10} Pa, and e is coupling matrix in C/m^2 [43], [44]. The shim was made of phosphor bronze with density 8780 kg/m^3 and following mechanical parameters

$$E_s = \begin{bmatrix} 17 & 8.8 & 8.8 & 0 & 0 & 0 \\ 8.8 & 17 & 8.8 & 0 & 0 & 0 \\ 8.8 & 8.8 & 17 & 0 & 0 & 0 \\ 0 & 0 & 0 & 8.2 & 0 & 0 \\ 0 & 0 & 0 & 0 & 8.2 & 0 \\ 0 & 0 & 0 & 0 & 0 & 8.2 \end{bmatrix} \quad (5)$$

where E_s is stiffness matrix in 10^{10} Pa.

Whereas known analytical relationships between the geometric parameters in (2) were used as initial guidelines for the PB design, only a few studies have reported on the breakdown voltage of PZT layers [45], [46], which is extremely important for the current study due to the intended long-term operation of the PB under a relatively high DC voltage. As such, the PZT electric field strength was kept below 1.5 kV/mm. Furthermore, ultra-thin benders that produce large displacement also produce insufficient force and are difficult to manufacture due to potential cracking during fabrication and higher susceptibility to mechanical stresses and vibration in industrial operating environment [47]. Therefore, PZT layers no less than 0.2 mm wide and a metal shim 0.15 mm wide were analyzed to ensure that the breakdown voltage would not be exceeded even under 300 VDC and the designed system was relatively simple to manufacture.

Table 1 summarizes the FEA results and shows that for the fixed heights of the PZT layers, the length of the PB should be increased considerably to ensure a sufficiently large δ_{tip}. Therefore, the PBs with a total length exceeding 50 mm can be expected to provide a $\delta_{tip} > 1$ mm. However, the application of the PB can be unreliable if a slight change in the applied voltage results in a dramatic decrease in δ_{tip}. On the other hand, extremely long PBs would result in unnecessary increase in size and price of PB and PES. Thus, a 70 mm long PB is the most promising candidate for application in a PES. The 10 mm difference in PZT layer and shim lengths in Table 1 aims to provide PZT-free space for fixing the PB to housing and allocating the moving wire of PES on the shim.

C. EXPERIMENTAL FEASIBILITY VERIFICATION OF THE DESIGNED PB

Table 2 summarizes the parameters of the fabricated PBs labeled PB55 and PB70. The PB prototypes were manufactured in collaboration with Dong-Il Technology Ltd., South Korea [47]. Fig. 5 shows the experimental setup with a PB and a Keyence LK-35 high-precision laser position sensor ensuring ±0.05% accuracy for the position measurement. The experiments were conducted in the 0–300 VDC range using a controlled DC voltage source. This range corresponds to the intended operating conditions of the PBs.

TABLE 1. FEA results for δ_{tip} in mm of bimorph PBs with h_p = 0.2 mm, h_s = 0.15 mm obtained using JMAG.

l_s, mm	l_p, mm	V_{dc}			
		60 V	120 V	200 V	300 V
30	20	0.03	0.07	0.11	0.17
40	30	0.09	0.19	0.31	0.46
55	45	0.26	0.51	0.91	1.31
70	60	0.56	1.1	1.76	2.78

TABLE 2. Parameters of the fabricated large tip displacement PBs.

Specimen	l_s, mm	l_p, mm	a_s, mm	h_p, mm	h_s, mm	C_{pb}, nF
PB55	55	45	5	0.2	0.15	14.6
PB70	70	60	5	0.2	0.15	18.1

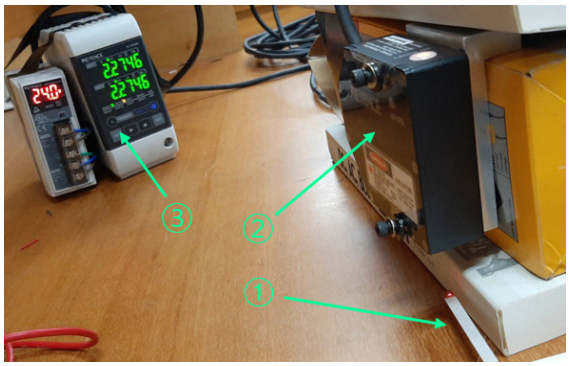

FIGURE 5. PB70 (1) displacement measurement setup including a Keyence LK-35 laser sensor head (2) and a power and measurement unit (3).

Fig. 6 shows that the PB55 and PB70 specimens both exhibited a near perfect linear response, which is beneficial because otherwise the complex means of mitigating nonlinearity and hysteresis are required [48], [49]. Most importantly, the PBs maintain their performance at relatively high voltages, indicating that the breakdown voltage of the PZT layers was not reached and the PBs can be reliably utilized in conventional power grids. Furthermore, the large displacement achieved, particularly for PB70, indicates that the designed PBs can provide sufficient macroscopic displacement to control low-weight external loads such as wires, to control a contact.

Fig. 6 also indicates that the designed PBs can sustain a considerable drop in voltage while maintaining a relatively large tip displacement. For example, PB70 provides more than 1 mm displacement even at 50% of the maximum DC voltage. On the other hand, upon removing the voltage the PBs were observed to return to their initial (relaxed) states, indicating that the relaxation of the PBs would result in closing the emergency circuit of the PES.

III. ZMC-PES SYSTEM ANALYSIS AND FEASIBILITY INVESTIGATION

A. DESIGN OF THE PROPOSED ZMC-PES SYSTEM

The studied ZMC-PES system shown in Fig. 7 includes a ZMC with two coils, both connected to a 220V/60Hz power

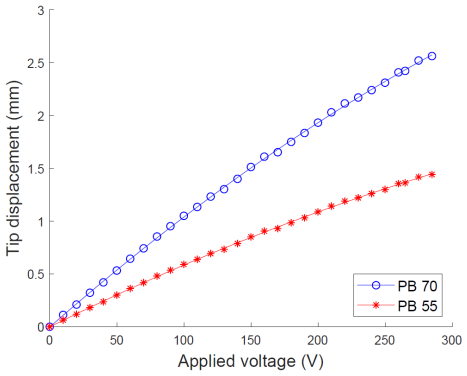

FIGURE 6. Experimental measurement of a PB response to DC voltage.

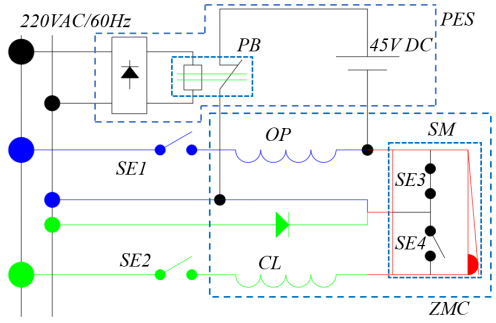

FIGURE 7. Electrical connection of the ZMC-PES system to the conventional power supply grid.

supply via two button switches labeled SE1 and SE2. There is an electromechanical switch, labeled SM, built into the ZMC that ensures that current can only flow in one of the coils at a time [12]. When the ZMC is closed, SE3 is closed and SE4 is open, meaning that only the opening coil (OP) can be energized; and when the ZMC is open, SE3 is open and SE4 is closed, so that only the closing coil (CL) is connected to the power supply (see Fig. 7).

The PES consists of a rectifier, a PB controlling a contact, and a 45 VDC battery. The PB reported in Section 2 is connected via a rectifier to the same AC power supply as the ZMC. Therefore, the state of the PB is coupled to the state of the power source rather than the state of the ZMC. The PB controls a contact in an emergency circuit connecting the OP to a 45 VDC battery (arranged as a series connection of five conventional 9 V batteries), bypassing the opening coil switch SE1 as shown in Fig. 7. The PB contact is normally closed, as the PB is relaxed at zero voltage and only deflected to open the contact when the rated voltage is applied. Hence, the emergency circuit is unused when the conventional power source is operating and the ZMC is controlled by the switches SE1 and SE2.

When the input voltage is removed, as in case of power outage, there are two possible scenarios for the PES connected to the ZMC:

1) The PES is connected when the ZMC is open. When ZMC is in the open state, connecting the battery to the OP has no effect because SE3 is open. Hence, the current flow is prevented and connecting the PES does not result in any kind of energy transfer.

2) The PES is connected when the ZMC is closed. The intended operation of the PES involves connecting it when the ZMC is closed. As shown in Fig. 8, in the absence of the PES, the ZMC remains closed when the AC voltage is removed. This is due to the PM holding force and the lack of power available to open it, posing a potential danger to the grid and personnel. However, Fig. 9 shows that connecting the PES results in opening the ZMC due to the current provided by the battery. When the ZMC is closed and the PES is connected, the OP is connected to the battery as shown in Fig. 7. When the ZMC is opened by the repulsion between the emergency opening current and the PM magnetic field, the SM disconnects the OP by opening SE3, ensuring that current does not continuously flow in the emergency circuit. Hence, the ZMC-PES is a zero-holding-energy system that acts as a normally-open MC.

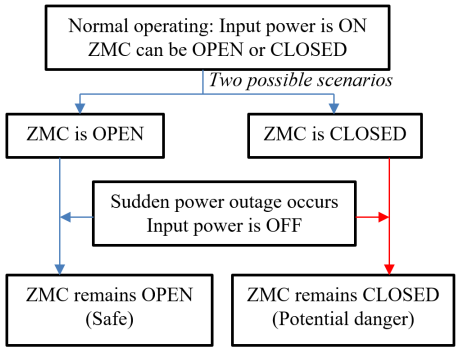

FIGURE 8. Response of ZMC in a sudden power outage scenario preserving its previous state.

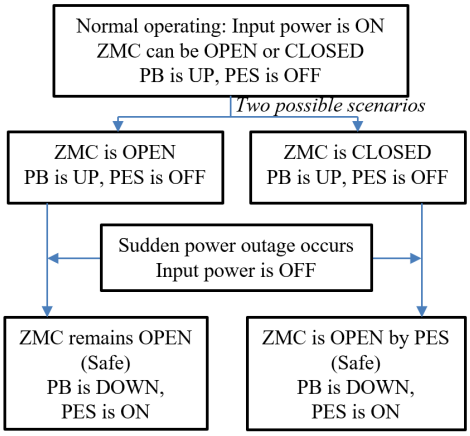

FIGURE 9. Emergency opening of ZMC by PES in the case of a power outage.

Table 3 summarizes the ZMC-PES emergency opening operation shown in Fig. 9, which can be described by the following steps:

TABLE 3. Description of the ZMC-PES emergency opening steps in case of a power outage.

Step	Input power	ZMC state	SE3 state	PB state	PES state	PES I_{op}, A	Time, ms
1	ON	1	1	Up	OFF	0	-
2	OFF	1	1	*Rel.*	OFF	0	0 10
3	OFF	1	1	Down	ON	0 0.5	10 30
4	OFF	1 0	1	Down	ON	0.5	30 50
5	OFF	0	0	Down	ON	0.5 0	50
6	OFF	0	0	Down	ON	0	>50

For states: 1 – closed, 0 – open; *Rel.* stands for relaxation

1) While input power is still ON, the ZMC is closed, the PB is UP, and the PES is disconnected (OFF).

2) When a power outage occurs, input power is cut OFF, the ZMC is still closed, but the PB starts relaxing. The PES is still disconnected.

3) Approximately 10 ms after the power outage, the PB reaches the DOWN position and the PES is connected. An emergency opening current then starts flowing in the opening coil of the ZMC.

4) Approximately 20 ms later the ZMC armature starts moving due to the repulsive force between the emergency current and PM.

5) Approximately 20 ms later the ZMC armature reaches the OPEN state, the SM disconnects the opening coil from the PES, and the current in the emergency circuit starts falling towards zero (see Fig. 14).

6) Approximately 50 ms after the blackout the emergency opening is finished, the emergency current is zero, the ZMC is in the open state and its load is disconnected. There is then no danger to personnel or the grid if the input power suddenly turns back on.

B. EXPERIMENTAL VALIDATION OF THE DEVELOPED ZMC-PES

Fig. 10 shows the experimental setup with a conventional AC network used as a power supply, corresponding to the diagram in Fig. 7. A Tektronix 4000 oscilloscope was used to measure the voltage and current waveforms as shown in Fig. 11.

The ZMC-PES verification experiment was conducted in the following manner. First, as the power was supplied to the ZMC and the PB switch via a rectifier, the PB70 moves a contact from the position shown in Fig. 12 (a) to the position in Fig. 12 (b), breaking the emergency circuit. Fig. 13 illustrates the same performance exhibited by PB55. Whereas the exact displacement of PBs was not measured during this experiment, Figs. 12 (b) and 13 (b) show visible mm-scale displacement produced by PBs under rectified AC voltage. With the PB up, the PES disconnected and power available, the ZMC can be operated normally using the button switches SE1 and SE2. In order to verify the emergency opening operation, the ZMC was closed using SE1 before the source voltage was removed. This resulted in the PB transitioning to a relaxed state and forming a contact between the moving and

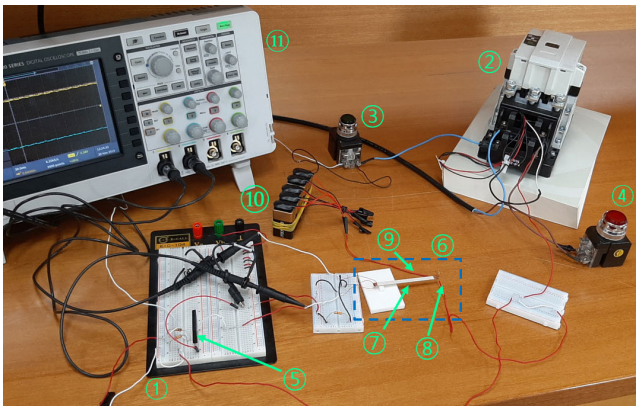

FIGURE 10. ZMC-PES experimental verification setup. The AC power is supplied at position (1) to the ZMC (2) and the PB switch (6) via a rectifier (5). The PB70 (7) moves a contact (8) to connect to a wire (9). The ZMCs normal operation is controlled by the switches *SE1* (3) and *SE2* (4). The PES battery (10) is connected to the *OP* of the ZMC. An oscilloscope (11) is used to measure the voltages and currents.

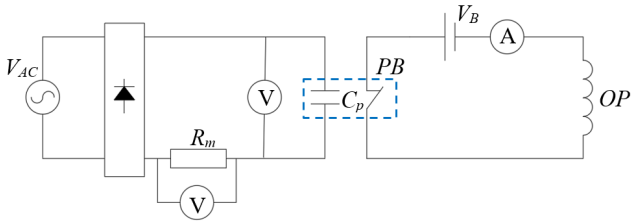

FIGURE 11. PES experimental circuit for the investigation of the rectified voltage waveform, current flow, and energy consumption.

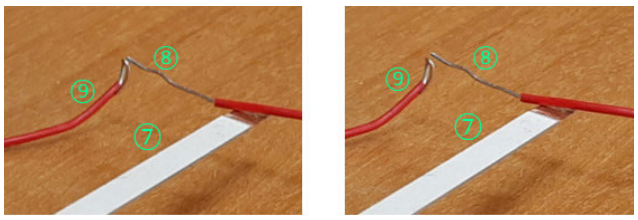

(a) (b)

FIGURE 12. PB70 (7) controls a contact made of a moving (8) and a stationary (9) wire in (a) closed state of PB switch during power outage and (b) open state corresponding to normal operation.

stationary wires, hence connecting the PES so that the battery was connected to the OP of the ZMC.

Figs. 12 and 13 also illustrate the negligible effect of wire weight on PB displacement in PES experiment. This is due to very thin wires used to conduct low transient PES current shown in Fig. 14. Fig. 14 also shows the corresponding ZMC armature displacement during the emergency opening when the battery is connected. As the ZMC opens, the OP is disconnected from the PES by the SM and the PES current drops to zero. Therefore, this experiment successfully verifies that PZT-ZMC system acts as a normally-open MC, which is essential for the safety and reliability of ZMC technology.

The results shown in Fig. 14 allow the emergency opening power consumption to be evaluated, which further translates to the number of times the emergency opening can be

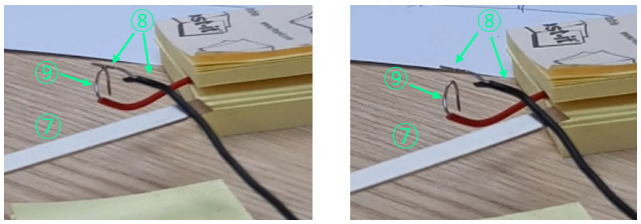

FIGURE 13. PB55 (7) controls contacts (8) and (9) in (a) closed and (b) open states of the PB switch.

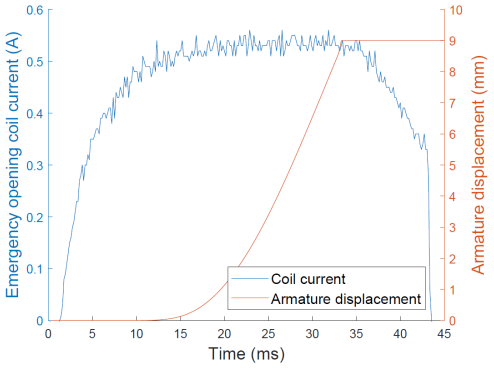

FIGURE 14. PES current and displacement of the ZMC armature during the emergency opening.

performed before the battery is drained, given by

$$N_e = \frac{W_b}{V_b I_e t_e} \tag{6}$$

where W_b is the total energy stored by the battery in J, V_b is battery voltage in V, I_e is emergency opening current in A, and t_e is the time over which the emergency current flows in s. Considering that a pack of five conventional 9 VDC batteries stores approximately 81 kJ of energy, the estimated Ne is 90000 operations. As the system is designed to operate only in emergency situations, this implies an extremely long lifetime.

C. VOLTAGE WAVEFORMS AND ENERGY CONSUMPTION OF THE PES

Fig. 15 shows that the PB decreases the oscillations in the rectified voltage by naturally acting as a capacitor. The experiment showed only a slight derivation from a perfectly constant value of the rectified DC voltage, which can be attributed to the ±5 V accuracy of the measurement unit for the measured 285 VDC signal level.

This measurement was also verified with a Fluke 177 multimeter, giving a result of 285±0.1 VDC. In order to estimate the energy consumption with a higher accuracy, the voltage drop V_m across a test resistor R_m (seen in Fig. 11) was measured, showing no measurable voltage above the 10 mV limit imposed by the measurement noise. This experiment allows an upper bound of the continuous current consumption of the PB to be given as shown in Table 4. Such a low upper

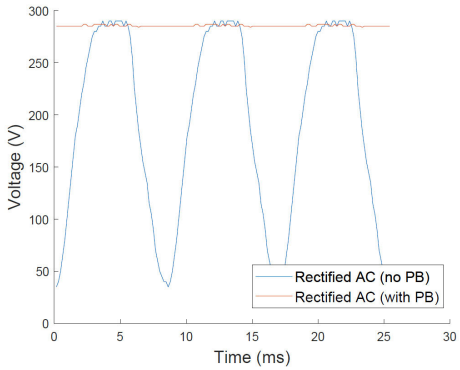

FIGURE 15. Effects of connecting the PB on the waveform of the rectified voltage.

TABLE 4. Estimated power consumption of the PES derived from experimental data.

V_{pb}, V	R_m, Ω	V_m, V	I_{pb}, mA	P_{pb}, μW
285	325	<10	<0.03	<0.3

bound of energy consumption essentially indicates that the PB does not consume any energy while deflected under a constant DC voltage, meaning that the entire PES subsystem also has zero continuous energy consumption. Energy loss (damping) associated with PB switching is also negligible due to rarity of extremely short switching operations and overall non-resonance operating conditions of the PB [50]. Therefore, the ZMC-PES is a zero-holding-energy system that acts as a normally-open MC in case of sudden power outage.

IV. DISCUSSION

A. COMPARISON OF THE PROPOSED ZMC-PES WITH CONVENTIONAL TECHNOLOGY

Table 5 shows a comparison between the main parameters of novel and conventional MCs. For reliability considerations, the reader is referred to the cited literature in Table 5. Notably, only ZMCs and the ZMC-PES have zero or nearly-zero holding energy consumption, P_h, in a closed state. On the other hand, conventional solenoid MCs and energy-saving PM MCs maintain an open state in the case of a power

TABLE 5. Comparison of power consumption and reliability of the conventional and proposed MCs.

MC type	P_h, W	P_h of 1000 MCs, W	Power outage state	Danger during power outage	Overall reliability
Solenoid MC [52]	10-20	10000-20000	Open	No	Low
PM MC [7], [56]	2-5	2000-5000	Open	No	Average
Electronic MC [11]	0.5	500	Open/ Closed	Yes	Low
ZMC [12]	0	0	Open/ Closed	Yes	Average
ZMC-PES	<0.3 10^{-6}	<0.3 10^{-6}	Open	No	High

outage and are not subjected to the reliability concerns described in this paper. However, their reliability is hindered by continuous vibration, heating, and a potential for contact welding [51].

Therefore, it is significant that the proposed ZMC-PES system solves the power outage scenario problem of ZMCs, while taking advantage of their superior performance as indicated by Table 5. Furthermore, Table 5 shows that the energy consumption accumulates when a facility operates numerous (e.g., 1000) contactors, except in the case of ZMCs. Moreover, the energy consumption of the ZMC-PES system does not necessarily increase with the number of ZMCs because a single PES can control multiple ZMCs as shown in Fig. 16. In this case the number of ZMCs only affects the lifetime of the battery. Replacing the battery is a more cost-effective solution compared to the expenses arising from the continuous energy consumption and maintenance costs of thousands of conventional MCs. Thus, the expenses associated with such systems can be reduced significantly by implementing the ZMC-PES.

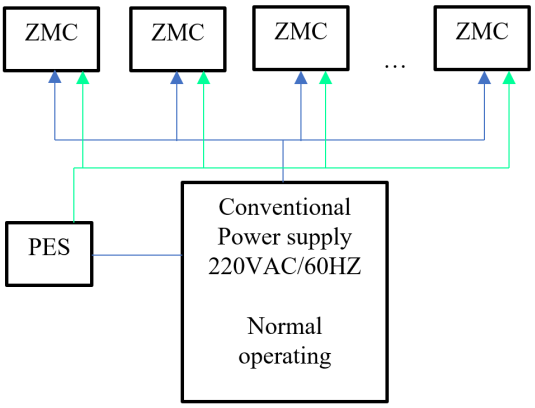

FIGURE 16. The possibility of operating multiples ZMCs with a single PES using conventional power supply.

B. OTHER APPLICATIONS OF THE DEVELOPED PES

Whereas the PES was proposed for controlling an AC ZMC in this paper, it can be used for DC contactors as well. Since DC is a necessary requirement for operating the PES, it will be naturally compatible with DC devices without requiring any rectification. Furthermore, an application of the PES in DC circuits is even more promising because the holding energy of DC MCs exceeds that of AC MCs [52].

In addition, the application of the PB proposed in this paper can be used for the development of a zero-holding-energy switch for DC grids. The PB switch can control low currents in response to the DC control voltage, while consuming no energy in either open or closed states. The PB also has a monitoring function, acting in response to the change in the applied voltage rather than a simplistic on/off operation. It should be noted that when connecting larger wires, or breaking non-zero current, the PB load should also be taken into account. Thus, wider PBs that produce larger forces can be generally recommended for such applications.

This makes the developed PB and PES-controlled PM MCs particularly promising for aircraft microgrids due to their ability to minimize the energy consumption with low-weight contactors or switches. Because aircraft microgrids utilize DC networks [53], [54] the application of the developed PB switch and PES will allow the fuel consumption to be reduced by substituting numerous conventional switches on an aircraft with the proposed technology. Furthermore, the same argument applies to electric ships that operate large sophisticated grids, where the reduction in energy consumption translates to increased battery lifetime and prolonged overall operating time of an electric vehicle [4], [55].

V. CONCLUSION

This paper proposes a PES that solves a critical safety problem of ZMCs in the event of a power outage, thus eliminating the main drawback in the implementation of ZMCs. This was achieved by incorporating a zero-holding-energy PB switch to monitor the input voltage and instantaneously connect the opening coil of the ZMC to an inexpensive battery in the event of a power outage, thereby leading to prompt opening and disconnection of the ZMC's load. The proposed ZMC-PES system acts as a normally open MC with zero holding energy. The feasibility of the proposed ZMC-PES system was confirmed using data obtained from a fabricated prototype, which verified the short response time and zero continuous energy consumption. The PB switch developed as part of the PES also showed potential as a zero-holding-energy control element for DC circuits, thus rendering it particularly suitable for autonomous vehicular microgrids and mechatronic devices. Comparisons of the ZMC-PES with traditional MC technology show its higher reliability and energy efficiency. Unlike traditional ZMCs, the proposed normally-open ZMC-PES system can be controlled using conventional solenoid MC control strategies, indicating the possibility of a convenient transition between conventional and future MC technologies. The proposed technology is particularly promising because it can be used by energy generation facilities, in distribution grids, and by end users. Moreover, the proposed ZMC-PES system can be installed in AC and DC vehicular microgrids to improve the energy-efficiency and lifetime of electric vehicles such as aircrafts and ships.

REFERENCES

[1] D. T. Danielson, *Barriers to Industrial Energy Efficiency. Report to Congress*. Washington, DC, USA: U.S. Dept. Energy, Jun. 2015.

[2] *United States Environmental Protection Agency (EPA)—Greenhouse Gas Emissions*. Accessed: Jun. 4, 2019. [Online]. Available: https://www.epa.gov/ghgemissions

[3] V. Madonna, P. Giangrande, and M. Galea, "Electrical power generation in aircraft: Review, challenges, and opportunities," *IEEE Trans. Transport. Electrific.*, vol. 4, no. 3, pp. 646–659, Sep. 2018, doi: 10.1109/TTE.2018.2834142.

[4] A. Accetta and M. Pucci, "Energy management system in DC micro-grids of smart ships: Main gen-set fuel consumption minimization and fault compensation," *IEEE Trans. Ind. Appl.*, vol. 55, no. 3, pp. 3097–3113, May 2019, doi: 10.1109/TIA.2019.2896532.

[5] F. A. Chachar, S. S. H. Bukhari, F. H. Mangi, D. E. Macpherson, G. P. Harrison, W. Bukhsh, and J.-S. Ro, "Hierarchical control implementation for meshed AC/Multi-terminal DC grids with offshore windfarms integration," *IEEE Access*, vol. 7, pp. 142233–142245, 2019, doi: 10.1109/ACCESS.2019.2944718.
[6] X. Liu, X. Wang, and J. Wen, "Optimal power flow of DC-grid based on improved PSO algorithm," *J. Electr. Eng. Technol.*, vol. 12, no. 4, pp. 1586–1591, 2017, doi: 10.5370/JEET.2017.12.4.1586.
[7] S. Fang, Q. Liu, H. Lin, and S. L. Ho, "A novel flux-weakening control strategy for permanent-magnet actuator of vacuum circuit breaker," *IEEE Trans. Ind. Electron.*, vol. 63, no. 4, pp. 2275–2283, Apr. 2016, doi: 10.1109/TIE.2015.2500182.
[8] L. Shu, L. Wu, G. Wu, and Z. Wu, "A fully coupled framework of predicting the dynamic characteristics of permanent magnet contactor," *IEEE Trans. Magn.*, vol. 52, no. 8, Aug. 2016, Art. no. 8001607, doi: 10.1109/TMAG.2016.2557310.
[9] Z. Wang, L. Sun, S. He, Y. Geng, and Z. Liu, "A permanent magnetic actuator for 126 kV vacuum circuit breakers," *IEEE Trans. Magn.*, vol. 50, no. 3, pp. 129–135, Mar. 2014, doi: 10.1109/TMAG.2013.2284251.
[10] Y. Han, W. Shang, C. Hou, A. Li, and Y. Cao, "Study on factors influencing the characteristics of arc in DC contactors," in *Proc. ICEPE-ST*, Dec. 2017, pp. 406–410, doi: 10.1109/ICEPE-ST.2017.8188886.
[11] H.-J. Bak, J.-S. Ro, T.-K. Chung, and H.-K. Jung, "Characteristics analysis and design of a novel magnetic contactor for a 220 V/85 a," *IEEE Trans. Magn.*, vol. 49, no. 11, pp. 5498–5506, Nov. 2013, doi: 10.1109/TMAG.2013.2268054.
[12] N. Gabdullin and J.-S. Ro, "Energy-efficient eco-friendly zero-holding-energy magnetic contactor for industrial and vehicular applications," *IEEE Trans. Veh. Technol.*, vol. 69, no. 5, pp. 5000–5011, May 2020, doi: 10.1109/TVT.2020.2981888.
[13] J.-G. Kim, "Reduction of inrush current and voltage drop by selecting optimum reactors in induction generators," *J. Electr. Eng. Technol.*, vol. 14, no. 2, pp. 693–700, Mar. 2019, doi: 10.1007/s42835-018-00061-1.
[14] Y. Luo, M. Dahmardeh, and K. Takahata, "Biocompatible circuit-breaker chip for thermal management of biomedical microsystems," *J. Micromech. Microeng.*, vol. 25, no. 5, May 2015, Art. no. 055002, doi: 10.1088/0960-1317/25/5/055002.
[15] B. Holz, H. Janocha, and L. Riccardi, "Compact MSM actuators—Concept for highest force exploitation," in *Proc. 13th Int. Conf. New Actuat., 7th Int. Exhib. Smart Actuat. Drive Syst.*, Bremen, Germany: WFB Wirtschaftsförderung Bremen, Division Messe Bremen, Jun. 2012, pp. 663–667.
[16] X. Tian, Q. Quan, L. Wang, and Q. Su, "An inchworm type piezoelectric actuator working in resonant state," *IEEE Access*, vol. 6, pp. 18975–18983, 2018, doi: 10.1109/ACCESS.2018.2814010.
[17] J. Nam, Y. Kim, and G. Jang, "Resonant piezoelectric vibrator with high displacement at haptic frequency for smart devices," *IEEE/ASME Trans. Mechatronics*, vol. 21, no. 1, pp. 394–401, Feb. 2016, doi: 10.1109/TMECH.2015.2452312.
[18] J. Nam, H. Oh, and G. Jang, "Externally leveraged resonant piezoelectric actuator with fast response time for smart devices," *IEEE/ASME Trans. Mechatronics*, vol. 21, no. 6, pp. 2764–2772, Dec. 2016, doi: 10.1109/TMECH.2016.2590564.
[19] X. D. Xie, Q. Wang, and N. Wu, "A ring piezoelectric energy harvester excited by magnetic forces," *Int. J. Eng. Sci.*, vol. 77, pp. 71–78, Apr. 2014, doi: 10.1016/J.IJENGSCI.2014.01.001.
[20] R. M. Toyabur, M. Salauddin, H. Cho, and J. Y. Park, "A multimodal hybrid energy harvester based on piezoelectric-electromagnetic mechanisms for low-frequency ambient vibrations," *Energy Convers. Manage.*, vol. 168, pp. 454–466, Jul. 2018, doi: 10.1016/j.enconman.2018.05.018.
[21] L. Wang, T. Tan, Z. Yan, D. Li, B. Zhang, and Z. Yan, "Integration of tapered beam and four direct-current circuits for enhanced energy harvesting from transverse galloping," *IEEE/ASME Trans. Mechatronics*, vol. 24, no. 5, pp. 2248–2260, Oct. 2019, doi: 10.1109/TMECH.2019.2932467.
[22] C.-L. Yang, K.-W. Chen, and C.-D. Chen, "Model and characterization of a press-button-type piezoelectric energy harvester," *IEEE/ASME Trans. Mechatronics*, vol. 24, no. 1, pp. 132–143, Feb. 2019, doi: 10.1109/TMECH.2018.2876007.
[23] Y. Fan and U.-X. Tan, "Design of a feedforward-feedback controller for a piezoelectric-driven mechanism to achieve high-frequency nonperiodic motion tracking," *IEEE/ASME Trans. Mechatronics*, vol. 24, no. 2, pp. 853–862, Apr. 2019, doi: 10.1109/TMECH.2019.2899069.
[24] D. Zhang, P. Li, J. Zhang, H. Chen, K. Guo, and M. Ni, "Design and assessment of a 6-DOF Micro/Nanopositioning system," *IEEE/ASME Trans. Mechatronics*, vol. 24, no. 5, pp. 2097–2107, Oct. 2019, doi: 10.1109/TMECH.2019.2931619.
[25] Z. Wen, Y. Ding, P. Liu, and H. Ding, "An efficient identification method for dynamic systems with coupled hysteresis and linear dynamics: Application to piezoelectric-actuated nanopositioning stages," *IEEE/ASME Trans. Mechatronics*, vol. 24, no. 1, pp. 326–337, Feb. 2019, doi: 10.1109/TMECH.2019.2891777.
[26] S. Akhbari, F. Sammoura, B. Eovino, C. Yang, and L. Lin, "Bimorph piezoelectric micromachined ultrasonic transducers," *J. Microelectromech. Syst.*, vol. 25, no. 2, pp. 326–336, Apr. 2016, doi: 10.1109/JMEMS.2016.2516510.
[27] G.-Y. Gu, L.-M. Zhu, C.-Y. Su, H. Ding, and S. Fatikow, "Modeling and control of piezo-actuated nanopositioning stages: A survey," *IEEE Trans. Autom. Sci. Eng.*, vol. 13, no. 1, pp. 313–332, Jan. 2016, doi: 10.1109/TASE.2014.2352364.
[28] J. Gao and Y. Altintas, "Development of a three-degree-of-freedom ultrasonic vibration tool holder for milling and drilling," *IEEE/ASME Trans. Mechatronics*, vol. 24, no. 3, pp. 1238–1247, Jun. 2019, doi: 10.1109/TMECH.2019.2906904.
[29] H. Nouraei, R. Ben-Mrad, and A. N. Sinclair, "Development of a piezoelectric fuel injector," *IEEE Trans. Veh. Technol.*, vol. 65, no. 3, pp. 1162–1170, Mar. 2016, doi: 10.1109/TVT.2015.2410136.
[30] P. Firoozy, S. E. Khadem, and S. M. Pourkiaee, "Broadband energy harvesting using nonlinear vibrations of a magnetopiezoelastic cantilever beam," *Int. J. Eng. Sci.*, vol. 111, pp. 113–133, Feb. 2017, doi: 10.1016/J.IJENGSCI.2016.11.006.
[31] Z. Butt, Z. Anjum, A. Sultan, F. Qayyum, H. M. K. Ali, and S. Mehmood, "Investigation of electrical properties & mechanical quality factor of piezoelectric material (PZT-4A)," *J. Electr. Eng. Technol.*, vol. 12, no. 2, pp. 846–851, Mar. 2017, doi: 10.5370/JEET.2017.12.2.846.
[32] O. Wunnicke and K. Reimann, "Piezoelectric biomorph switch," U.S. Patent 8 847 466 B2, Sep. 30, 2014.
[33] S. Zheng, M. Chen, Z. Li, and H. Wang, "Size-dependent constituent equations of piezoelectric bimorphs," *Compos. Struct.*, vol. 150, pp. 1–7, Aug. 2016, doi: 10.1016/j.compstruct.2016.04.039.
[34] N. Chen, P. Yan, and J. Ouyang, "A generalized approach on bending and stress analysis of beams with piezoelectric material bonded," *Sens. Actuators A, Phys.*, vol. 290, pp. 54–61, May 2019, doi: 10.1016/j.sna.2019.02.029.
[35] S. Khadraoui, M. Rakotondrabe, and P. Lutz, "Optimal design of piezoelectric cantilevered actuators with guaranteed performances by using interval techniques," *IEEE/ASME Trans. Mechatronics*, vol. 19, no. 5, pp. 1660–1668, Oct. 2014, doi: 10.1109/TMECH.2013.2292494.
[36] S. Zarif Mansour, R. J. Seethaler, Y. R. Teo, Y. K. Yong, and A. J. Fleming, "Piezoelectric bimorph actuator with integrated strain sensing electrodes," *IEEE Sensors J.*, vol. 18, no. 14, pp. 5812–5817, Jul. 2018, doi: 10.1109/JSEN.2018.2842138.
[37] N. Gabdullin and J.-S. Ro, "Novel non-linear transient path energy method for the analytical analysis of the non-periodic and non-linear dynamics of electrical machines in the time domain," *IEEE Access*, vol. 7, pp. 37833–37854, 2019, doi: 10.1109/ACCESS.2019.2905856.
[38] K. Uchino, *Piezoelectric Actuators and Ultrasonic Motors*. New York, NY, USA: Springer, 1997, ch. 4, p. 137.
[39] J. Liu, Y. Liu, L. Zhao, D. Xu, W. Chen, and J. Deng, "Design and experiments of a single-foot linear piezoelectric actuator operated in a stepping mode," *IEEE Trans. Ind. Electron.*, vol. 65, no. 10, pp. 8063–8071, Oct. 2018, doi: 10.1109/TIE.2018.2798627.
[40] B.-W. Kang and J. Kim, "Design, fabrication, and evaluation of stepper motors based on the piezoelectric torsional actuator," *IEEE/ASME Trans. Mechatronics*, vol. 18, no. 6, pp. 1850–1854, Dec. 2013, doi: 10.1109/TMECH.2013.2269171.
[41] Y. Q. Fu, J. K. Luo, N. T. Nguyen, A. J. Walton, A. J. Flewitt, X. T. Zu, Y. Li, G. McHale, A. Matthews, E. Iborra, H. Du, and W. I. Milne, "Advances in piezoelectric thin films for acoustic biosensors, acoustofluidics and lab-on-chip applications," *Prog. Mater. Sci.*, vol. 89, pp. 31–91, Aug. 2017, doi: 10.1016/j.pmatsci.2017.04.006.
[42] M. Kimura, A. Ando, D. Maurya, and S. Priya, "Lead zirconate titanate-based piezoceramics," in *Advanced Piezoelectric Materials*, 2nd ed. Cambridge, U.K.: Woodhead Publishing, 2017, pp. 95–126.
[43] M. G. R. Sause and S. Richler, "Finite element modelling of cracks as acoustic emission sources," *J. Nondestruct. Eval.*, vol. 34, no. 1, Mar. 2015, doi: 10.1007/s10921-015-0278-8.
[44] M. G. R. Sause, M. A. Hamstad, and S. Horn, "Finite element modeling of conical acoustic emission sensors and corresponding experiments," *Sens. Actuators A, Phys.*, vol. 184, pp. 64–71, Sep. 2012, doi: 10.1016/j.sna.2012.06.034.

[45] M. Lebedev and J. Akedo, "What thickness of the piezoelectric layer with high breakdown voltage is required for the microactuator?" *Jpn. J. Appl. Phys.*, vol. 41, no. 1, pp. 3344–3347, May 2002, doi: 10.1143/jjap.41.3344.
[46] L. Graber, S. Smith, D. Soto, I. Nowak, J. Owens, and M. Steurer, "A new class of high speed disconnect switch based on piezoelectric actuators," in *Proc. IEEE Electr. Ship Technol. Symp. (ESTS)*, Jun. 2015, pp. 312–317, doi: 10.1109/ESTS.2015.7157910.
[47] Dong-Il Technologies. *Piezoelectric Transducers*. Accessed: Jun. 12, 2020. [Online]. Available: http://www.dongiltech.co.kr/
[48] J. A. Mynderse and G. T.-C. Chiu, "Two-degree-of-freedom hysteresis compensation for a dynamic mirror actuator," *IEEE/ASME Trans. Mechatronics*, vol. 21, no. 1, pp. 29–37, Feb. 2016, doi: 10.1109/TMECH.2015.2493038.
[49] N. Bajaj, A. B. Sabater, J. N. Hickey, G. T.-C. Chiu, and J. F. J. Rhoads, "Design and implementation of a tunable, duffing-like electronic resonator via nonlinear feedback," *J. Microelectromech. Syst.*, vol. 25, no. 1, pp. 2–10, Feb. 2016, doi: 10.1109/JMEMS.2015.2493447.
[50] D. A. DeAngelis and G. W. Schulze, "The effects of piezoelectric ceramic dissipation factor on the performance of ultrasonic transducers," *Phys. Procedia*, vol. 63, pp. 28–36, Jan. 2015, doi: 10.1016/j.phpro.2015.03.005.
[51] J. Jebramcik and F. Berger, "Investigations on the make-welding behavior of high power contactors for AC and DC applications up to 3kV," in *Proc. Annu. Holm Conf. Electr. Contacts*, Clearwater Beach, FL, USA, Dec. 2016, pp. 228–232, doi: 10.1109/HOLM.2016.7780037.
[52] *TeSys Catalogue Motor Control and Protection Components*, Schneider Electric, Rueil-Malmaison, France, 2019.
[53] J. Brombach, T. Schroter, A. Lucken, and D. Schulz, "Optimized cabin power supply with a / 270 v DC grid on a modern aircraft," in *Proc. 7th Int. Conf.-Workshop Compat. Power Electron. (CPE)*, Jun. 2011, pp. 425–428, doi: 10.1109/CPE.2011.5942274.
[54] B. Sarlioglu and C. T. Morris, "More electric aircraft: Review, challenges, and opportunities for commercial transport aircraft," *IEEE Trans. Transport. Electrific.*, vol. 1, no. 1, pp. 54–64, Jun. 2015, doi: 10.1109/TTE.2015.2426499.
[55] X. Feng, K. L. Butler-Purry, and T. Zourntos, "Real-time electric load management for DC zonal all-electric ship power systems," *Electr. Power Syst. Res.*, vol. 154, pp. 503–514, Jan. 2018, doi: 10.1016/j.epsr.2017.09.014.
[56] Schneider Electric. *NEMA Contactors and Starters*. Accessed: Oct. 10, 2019. [Online]. Available: https://www.se.com/ca/en/product-subcategory/86945-nema-contactors-and-starters/

NIKITA GABDULLIN (Member, IEEE) received the B.S. and M.S. degrees in electrical engineering from National Research University MPEI, Moscow, Russia, in 2010 and 2012, respectively, and the Ph.D. degree in electrical and electronic engineering from the City, University of London, London, U.K., in 2017. He is currently a Postdoctoral Researcher with Chung-Ang University, Seoul, South Korea. His research interests include analytical and numerical modeling of electromagnetic fields, novel electrical machine design, multiphysics and coupled problem analysis, application of piezoelectric, magnetic shape memory, and other smart materials in energy-efficient electromagnetic devices.

JONG-SUK RO (Member, IEEE) received the B.S. degree in mechanical engineering from Hanyang University, Seoul, South Korea, in 2001, and the Ph.D. degree in electrical engineering from Seoul National University (SNU), Seoul, in 2008. He has conducted Research with the Research and Development Center, Samsung Electronics, as a Senior Engineer, from 2008 to 2012. From 2012 to 2013, he was with the Brain Korea 21 Information Technology, SNU, as a Postdoctoral Fellow. He has conducted Research with the Electrical Energy Conversion System Research Division, Korea Electrical Engineering and Science Research Institute, as a Researcher, in 2013. From 2013 to 2016, he was with the Brain Korea 21 Plus, SNU, as a BK Assistant Professor. In 2014, he was with the University of Bath, Bath, U.K. He is currently an Associate Professor with the School of Electrical and Electronics Engineering, Chung-Ang University, Seoul.